Effective four-dimensional loop quantum black hole with a cosmological constant

Jianhui Lin and Xiangdong Zhang[*]

Department of Physics, South China University of Technology, Guangzhou 510641, China

In this paper, we utilize the effective corrections of the $\bar{\mu}$ scheme in loop quantum black holes to obtain a four-dimensional spherically symmetric metric with a cosmological constant. By imposing the areal gauge on the components of Ashtekar variables in the classical theory and applying the holonomy corrections, we derive the equations of motion, which can be solved to obtain the expression for the effective metric in the Painlevé-Gullstrand coordinates. Compared to the classical de Sitter (anti–de Sitter) spacetime, the loop quantum gravity (LQG) correction sets an upper bound on the cosmological constant as $\Lambda < \frac{3}{\gamma^2 \Delta}$. The thermodynamic properties of black holes have also been calculated. We interestingly found that for a small black hole, the temperature of the LQG black hole decreases as the mass decreases, which is quite different with the classical scenario. Moreover, our result shows that a logarithmic term appeared as the leading order correction to the Beikenstein-Hawking entropy. Furthermore, the LQG corrections also introduce an extra phase transition in the black hole's heat capacity at smaller radius.

I. INTRODUCTION

The prediction of the singularity at the center of black holes by classical general relativity (GR) has led to the widespread belief that classical theory has limitations and that quantum gravity effects need to be introduced to cure this type of spacetime singularity. Pursuing a consistent quantum gravity theory becomes one of the greatest challenges since the twentieth century.

One approach to investigating how quantum gravity affects the spacetime of black holes is to start with a specific quantum gravity theory and determine its model corresponding to spherically symmetric spacetime, and then make physical predictions based on the model. Loop quantum gravity (LQG) is currently one of the candidates for a theory of quantum gravity. As a background independent and nonperturbative theory, it has considerable appeal in this regard (see, e.g., [1–4]). Since the late 1980s, LQG based on Ashtekar variables has seen significant development up to the present day. This includes natural predictions for discrete geometrical spectrum [5–10] and successful generalizations to metric $f(R)$ theories, higher-dimensional gravity and so on [11–13]. It preserves two fundamental principles of general relativity: diffeomorphism invariance and background independence. The construction of LQG adheres to mathematical rigor and physical self-consistency. In situations where current experimental conditions cannot be satisfied, it is necessary to theoretically consider whether the classical limit of quantum theory is correct.

The application of LQG to cosmology, known as loop quantum cosmology (LQC), has been established as an appropriate semiclassical state [14], and the expectation values of the quantum operators in this state match well with their corresponding classical values. It has also led to the conclusion that the "big bounce" replaces the big bang, successfully resolving the problem of the cosmological singularity of the big bang [15–17]. LQC is the symmetry-reduced model of LQG [18]. In the classical scenario, before quantization, we can utilize the symmetries of spatial homogeneity and isotropy to reduce the phase space of gravitational degrees of freedom from infinite dimensions to finite dimensions. Then, by using the methods and techniques of LQG, it is able to proceed with its quantization. For a detailed review of LQC, see, e.g., [19,20].

Due to the success of LQC in resolving classical cosmological puzzles, the attempt to apply this technique to black holes to address the issue of black hole singularity is a very intriguing idea. As the simplest black hole solution, the Schwarzschild black hole then serves as an ideal arena to implement these ideas. Note that the interior of Schwarzschild black hole is isometric to the Kantowski-Sachs model [17,21], thus allowing for the potential adaptation of techniques and ideas from LQC. Therefore, in the past decade or so, the exploration of loop quantum black hole models has been a popular direction [17,21–25].

Since the success of LQC is based on its unique $\bar{\mu}$ quantization scheme. It is therefore great interest to also

[*]Contact author: scxdzhang@scut.edu.cn

implement the $\bar{\mu}$ scheme in loop quantum black hole models. In the quantum effective Hamiltonian constraint, the holonomy correction is simplified by replacing the components of the Ashtekar connection with quantum corrections, which are controlled by the quantum regularization parameters due to the fundamental discreteness of LQG. In the $\bar{\mu}$ scheme, the quantum parameters are chosen as adaptive discreteness variables. However, the $\bar{\mu}$-scheme encounters an issue of excessive quantum corrections at the event horizon [26]. In the classical regime, excessive quantum corrections are generally considered unacceptable. Moreover, in [27], the unimodular formulation of general relativity is proposed to study the full quantum dynamics of the LQC and the unimodular representation is applied to the homogeneous black hole interior spacetime such that we can test the various regularization schemes. It is showed that in $\bar{\mu}$ scheme, the area of the 2-sphere is smaller than the area gap in LQG, which violates the very construction of the $\bar{\mu}$ scheme. Fortunately, recently, as suggested by some authors [28], the reason of traditional $\bar{\mu}$ scheme cannot be implemented is simply because we choose the wrong set of coordinates which becomes null at the horizon. Hence they suggested to implement the $\bar{\mu}$ scheme in terms of another set of coordinates which will not become null at the horizon. The use of everywhere spacelike Painlevé-Gullstrand coordinates can be employed for the $\bar{\mu}$ scheme and avoid the aforementioned problem, leading to an effective framework for spherically symmetric vacuum solutions with holonomy corrections from loop quantum gravity [28].

On the other hand, up to now, most of the studies on loop quantum black hole models are limited to the Schwarzschild case. Note that our current Universe is undergoing an accelerating expansion and leading to the famous dark energy issue. The origin of dark energy remains as one of the biggest challenges to modern physics. Many possible mechanisms have been proposed to account for this issue, such as the phenomenological models [29], modified gravity [30–33], higher dimensions [34] and so on. Among them, the cosmological constant is generally believed as the most simplest explanation [33,35]. Though people may argue that the observed cosmological constant $\Lambda \approx 10^{-52}$ m^{-2} is so small and hence its effects can be safely ignored. However, the existence of a cosmological constant, regardless its value, will dramatically changed the asymptotic structure of the spacetime [36]. In addition, inspired by AdS/CFT correspondence, the black hole solutions with a negative cosmological constant also should be considered. Moreover, in Schwarzschild-AdS (anti–de Sitter) case, we have more richer physics such as Hawking-Page phase transition and the extended phase space thermodynamics can be established. Hence, the inclusion of a cosmological constant in a black hole solution is important both in the practical and the theoretical sense.

Additionally, thermodynamic properties of black holes have been studied for many years. Corresponding to the standard laws of thermodynamics, black hole thermodynamics also has four laws. Just like the standard laws of thermodynamics, black hole thermodynamics also follows four fundamental laws [37]. The first law, for example, establishes an energy conservation equation that connects the entropy of a black hole to its mass, charge, rotation, and other parameters [38]. As a thermodynamic system, black holes can be assessed for their thermodynamic stability. For instance, the Schwarzschild black hole, has a negative heat capacity, indicating that it is thermodynamically unstable. Also, it was discovered that the spacetime of black holes can exhibits a rich phase structure and critical phenomena (see, e.g., [39–41]), which are entirely similar to those found in other known thermodynamic systems. Within this context, if we aim to explore whether black holes exhibit phase transition behavior similar to that of a van der Waals fluid, we need to extend the metric to include a cosmological constant. This is because, in the extended phase space, the pressure is linked to the cosmological constant, which is no longer treated as a constant [39]. Therefore, to calculate the possible phase transition behavior of black holes in LQG, we must extend the effective metric to include a cosmological constant. Therefore, in this paper, we will follow the line of [28] by utilizing $\bar{\mu}$ scheme in Painlevé-Gullstrand coordinates to study the loop quantization of Schwarzschild–de Sitter (anti–de Sitter) black holes.

This paper will be organized as follows: We will start from the classical Hamiltonian framework and, in Sec. II, present the specific form of the metric using the components of connection and densitized triad as dynamical variables. In Sec. III, the LQG holonomy corrections are employed and obtain corresponding metric solutions. Additionally, a discussion of the physical properties of the solutions is provided in Sec. IV. Having obtained the effective metric with a cosmological constant, in Sec. V, we investigate the phase transitions behavior of AdS black holes in LQG. Finally, Sec. VI concludes the article with a summary.

Our conventions are the following: spacetime indices are denoted by $\mu, \nu, \rho, \sigma, \ldots$; spatial indices are denoted by $a; b; c; \ldots$; and internal indices are denoted by $i, j, k, ..$ We only set $c = 1$ but keep G and $\hbar$ explicit.

II. CLASSICAL THEORY

The metric of a four-dimensional spherically symmetric spacetime can be expressed in Painlevé-Gullstrand coordinates as

$$ds^2 = -N^2 dt^2 + f^2 (dx + N^x dt)^2 + y^2 d\Omega^2, \quad (1)$$

where the lapse N, shift vector N^x and f, y all are the function of time t and the radial coordinate x, while $d\Omega$,

given by $d\Omega^2 = d\theta^2 + \sin^2\theta d\phi^2$, is the line element on the unit sphere.

As the foundation of LQG, connection dynamics is a theory based on the Hamiltonian formulation of GR, described by Ashtekar-Barbero connections and their conjugate momentum in terms of triads. In loop quantum black hole models, we also inherit this feature and use them as basic variables. In this context, the basic variables are consistent with [28], which, respectively, are the Ashtekar-Barbero connection components given by $c(x)$, $p(x)$, and the densitized triad components given by $E^c(x)$, $E^p(x)$. The following represent the densitized triads in terms of metric components [28]

$$E_1^x = y^2 \sin\theta = E^c \sin\theta, \qquad E_2^\theta = fy \sin\theta = E^p \sin\theta,$$
$$E_3^\phi = fy = E^p. \tag{2}$$

Moreover, the Ashtekar-Barbero connection are written as $A_a^i = \Gamma_a^i + \gamma K_a^i$, where both the spin-connection Γ_a^i and the extrinsic curvature K_a^i only have three nonzero components [28]

$$K_x^1 = \frac{c}{\gamma}, \quad K_\theta^2 = \frac{p}{\gamma}, \quad K_\phi^3 = \frac{p\sin\theta}{\gamma},$$
$$\Gamma_\theta^3 = -\frac{\partial_x E^c}{2E^p}, \quad \Gamma_\phi^1 = -\cos\theta, \quad \Gamma_\phi^2 = \frac{\partial_x E^c \sin\theta}{2E^p}, \tag{3}$$

where γ is the Barbero-Immirzi parameter (a dimensionless constant that labels various inequivalent kinematic quantizations of LQG). The determinant of the spatial metric is $q = E^c(E^p \sin\theta)^2$.

A. Actions and constraints

The action of GR plus a cosmological constant reads

$$S = \frac{1}{16\pi G} \int d^4x \sqrt{-g}(R - 2\Lambda). \tag{4}$$

After performing canonical analysis, the gravitational action becomes

$$S = \int dt \int_\Sigma \left[\frac{\dot{A}_a^i E_i^a}{8\pi G\gamma} - N\mathcal{H}_\Lambda - N^a \mathcal{H}_a \right], \tag{5}$$

where the dot means the derivative with respect to time t; the Hamiltonian constraint $\mathcal{H}_\Lambda$ and the diffeomorphism constraints read, respectively, as

$$\mathcal{H}_\Lambda = -\frac{E_i^a E_j^b}{16\pi G\gamma^2 \sqrt{q}} \epsilon^{ij}{}_k (F_{ab}{}^k - (1 + \gamma^2)\Omega_{ab}{}^k)) - \frac{\sqrt{q}N}{8\pi G}\Lambda, \tag{6}$$

$$\mathcal{H}_a = \frac{1}{8\pi G\gamma} E_k^b F_{ab}{}^k. \tag{7}$$

Here the field strength is given by $F_{ab}{}^k = 2\partial_{[a}A_{b]}^k + \epsilon_{ij}{}^k A_a^i A_b^j$ and the spatial curvature denotes $\Omega_{ab}{}^k = 2\partial_{[a}\Gamma_{b]}^k + \epsilon_{ij}{}^k \Gamma_a^i \Gamma_b^j$. Due to the spherical symmetry, we can integrate over $d\Omega$ and use Eq. (2), then obtain the following expression

$$S = \int dt \int dx \left[\frac{\dot{c}E^c + 2\dot{p}E^p}{2G\gamma} - N\mathcal{H}_\Lambda - N^x \mathcal{H}_x \right], \tag{8}$$

where the Hamiltonian constraint reads

$$\mathcal{H}_\Lambda = -\frac{1}{2G\gamma}\left[\frac{2cp\sqrt{E^c}}{\gamma} + \frac{E^p}{\gamma\sqrt{E^c}}(p^2 + \gamma^2) - \frac{\gamma(\partial_x E^c)^2}{4E^p\sqrt{E^c}} \right.$$
$$\left. - \gamma\sqrt{E^c}\partial_x\left(\frac{\partial_x E^c}{E^p}\right) - \gamma\sqrt{E^c}E^p\Lambda \right], \tag{9}$$

and the diffeomorphism constraint is

$$\mathcal{H}_x = \frac{1}{2G\gamma}(2E^p\partial_x p - c\partial_x E^c). \tag{10}$$

Here straightforward calculations show only that $\mathcal{H}_x$ is nonzero and $\mathcal{H}_\theta, \mathcal{H}_\phi$ both vanish. Moreover, from Eq. (8), the symplectic structure of the symmetry-reduced black hole models is given by

$$\{c(x_1), E^c(x_2)\} = 2G\gamma\delta(x_1 - x_2), \tag{11}$$

$$\{p(x_1), E^p(x_2)\} = G\gamma\delta(x_1 - x_2), \tag{12}$$

with δ being the Dirac delta function. We now consider the smeared constraint function $\mathcal{C}[N] = \int dx N\mathcal{H}_\Lambda$ and $\mathcal{D}[N^x] = \int dx N^x \mathcal{H}_x$. Through lengthy but straightforward calculations, the Poission brackets between constraints algebra read

$$\{\mathcal{C}[N_1], \mathcal{C}[N_2]\} = \mathcal{D}\left[\frac{E^c}{(E^p)^2}(N_1\partial_x N_2 - N_2\partial_x N_1) \right], \tag{13}$$

$$\{\mathcal{D}[N_1^x], \mathcal{D}[N_2^x]\} = \mathcal{D}[(N_2^x\partial_x N_1^x - N_1^x\partial_x N_2^x)], \tag{14}$$

$$\{\mathcal{C}[N], \mathcal{D}[N^x]\} = -\mathcal{C}[N^x\partial_x N]. \tag{15}$$

As compared to the case without the cosmological constant [28], the symplectic structure and the constraint algebra have not changed. Using the Hamilton evolution equations $\dot{y} = \{y, \mathcal{C}[N] + \mathcal{D}[N^x]\}$, the equations of motion for each component with respect to time are determined by

$$\dot{E}^c = \frac{2Np}{\gamma}\sqrt{E^c} + N^x\partial_x E^c, \tag{16}$$

$$\dot{E}^p = \frac{N}{\gamma\sqrt{E^c}}(cE^c + pE^p) + \partial_x(N^x E^p), \tag{17}$$

$$\dot{c} = \frac{N}{2\gamma\sqrt{E^c}} \left[\frac{E^p}{E^c}(p^2 + \gamma^2) - 2cp \right] + \gamma\partial_x\left(\frac{\partial_x(N\sqrt{E^c})}{E^p}\right)$$
$$+ \frac{N\gamma}{2\sqrt{E^c}}\left[\partial_x\left(\frac{\partial_x E^c}{E^p}\right) - \frac{(\partial_x E^c)^2}{4E^c E^p}\right] + \partial_x(N^x c)$$
$$- \frac{\gamma}{2}\partial_x\left(N\frac{\partial_x E^c}{E^p\sqrt{E^c}}\right) + \frac{N\gamma E^p\Lambda}{2\sqrt{E^c}}, \tag{18}$$

$$\dot{p} = -\frac{N}{2\gamma\sqrt{E^c}}(p^2 + \gamma^2) - \frac{\gamma}{2}\left[\frac{N}{\sqrt{E^c}}\left(\frac{\partial_x E^c}{2E^p}\right)^2\right.$$
$$\left. - \partial_x(N\sqrt{E^c})\frac{\partial_x E^c}{(E^p)^2} + N^x\partial_x c\right] + \frac{N\gamma\sqrt{E^c}\Lambda}{2}. \tag{19}$$

Once the lapse and shift vector are chosen, by solving the above equations of motion and the diffeomorphism constraint together with the Hamiltonian constraint, one can obtain the vacuum spherically symmetric metric with the cosmological constant.

B. Classical solutions

Following the same approach in [28], we also adapt the areal gauge for E^c as follows:

$$E^c = x^2. \tag{20}$$

Once the areal gauge is imposed, the diffeomorphism constraint (10) then in turn implies

$$c = \frac{E^p}{x}\partial_x p. \tag{21}$$

The gauge-fixing condition $\zeta = E^c - x^2$ is second class with the diffeomorphism constraint $\mathcal{H}_x$, which should be preserved by the equations of motion. That is to say, $\dot{\zeta} = 0$. Using the condition $\dot{E}^c = 0$, we can obtain the expression

$$N^x = -\frac{Np}{\gamma}, \tag{22}$$

which implies that N^x is no longer a Lagrange multiplier. After choosing the areal gauge, N^x is determined by the lapse function N. Through this process, the action can be simplified and given by

$$S_{\text{GF}} = \int dt \int dx \left[\frac{\dot{p}E^p}{G\gamma} - N\mathcal{H}_\Lambda\right], \tag{23}$$

with

$$\mathcal{H}_\Lambda = \frac{1}{2G\gamma}\left[\frac{3\gamma x}{E^p} - \frac{2\gamma x^2}{(E^p)^2}\partial_x E^p - \frac{E^p}{\gamma x}\partial_x[x(p^2 + \gamma^2)]\right]$$
$$+ \frac{xE^p}{2G}\Lambda. \tag{24}$$

Since the E^c is fixed by the areal gauge, the remaining symplectic structure of the symmetry-reduced theory reads

$$\{p(x_1), E^p(x_2)\} = G\gamma\delta(x_1 - x_2), \tag{25}$$

and similarly, the remaining constraint algebra is

$$\{\mathcal{C}[N_1], \mathcal{C}[N_2]\} = C\left[-\frac{1}{\gamma}(N_1\partial_x N_2 - N_2\partial_x N_1)p\right],$$
$$= C[N_1^x\partial_x N_2 - N_2^x\partial_x N_1], \tag{26}$$

where the second step utilizes Eq. (22), which corresponds to the Painlevé-Gullstrand coordinates. The equations of motion can also be simplified to

$$\dot{E}^p = \frac{p}{\gamma x}(NE^p - x\partial_x(NE^p)), \tag{27}$$

$$\dot{p} = \frac{\gamma Nx}{2(E^p)^2} + \frac{\gamma x^2}{(E^p)^2}\partial_x N - \frac{N}{2x\gamma}\partial_x(xp^2 + \gamma^2 x) + \frac{\gamma Nx}{2}\Lambda, \tag{28}$$

which can be obtained by substituting areal gauge (20) and the expression (22) into the equations of motion (17) and (19). Now we set $N = 1$, and take into account the Hamiltonian constraint $\mathcal{H}_\Lambda = 0$. Then, $\dot{E}^p = 0$ and $\dot{p} = 0$ can be solved to obtain

$$E^p = C_1 x, \tag{29}$$

$$p^2 = \gamma^2\left(\frac{1}{C_1^2} - 1\right) + \frac{\gamma^2 x^2\Lambda}{3} + \frac{C_2}{x}, \tag{30}$$

where C_1 and C_2 are two constants of integration. Furthermore, these solutions (29) and (30) satisfy the Hamiltonian constraint equation $\mathcal{H}_\Lambda = 0$ identically. From Eq. (2), it is worthy noting that both f and y can be expressed in terms of E^c and E^p with

$$f^2 = \frac{(E^p)^2}{E^c}, \tag{31}$$

$$y^2 = E^c. \tag{32}$$

Using the Eqs. (22), (31), (32) and $N = 1$, by inserting the solutions (29) and (30) into the metric (1), we obtain

$$ds^2 = -\left(1 - \frac{2GM}{x} - \frac{x^2\Lambda}{3}\right)dt^2$$
$$+ 2\sqrt{\frac{2GM}{x} + \frac{x^2\Lambda}{3}}dxdt + dx^2 + x^2 d\Omega^2, \tag{33}$$

where we can determine the integration constants $C_1 = 1$ and $C_2 = 2GM\gamma^2$ by comparing with the standard

Schwarzschild–de Sitter (anti–de Sitter) solution and M is the mass of the black hole. Moreover, we can also confirm that the square root of p is negative. Finally, the solutions to the equations of motion are given by

$$E^p = x, \tag{34}$$

$$p = -\sqrt{\frac{2GM\gamma^2}{x} + \frac{\gamma^2 x^2 \Lambda}{3}}. \tag{35}$$

III. EFFECTIVE CORRECTION OF LQG

We adopt the standard LQC treatment for Schwarzschild black holes, which requires to introduce holonomy corrections. The holonomy of an $SU(2)$ connection A_a^i is a path-ordering exponential integral along an edge e^a

$$h(A) = \mathcal{P} \exp \int_{e_i} dt A_a^j \tau_j e^a, \tag{36}$$

with $\mathcal{P}$ labeling path ordering. Although it is not yet fully clear whether the LQG dynamics of a loop quantum Schwarzschild black hole can also provide a good approximation for the full LQG dynamics of the Schwarzschild black hole spacetime, the success of LQC has led people to believe that the effective dynamics of the loop quantum Schwarzschild black hole model can serve as a good approximation for the semiclassical quantum dynamics of observable objects with physical length scales much larger than the Planck scale. As the basic operators in LQG are the holonomies and triads, it is necessary to use the holonomies instead of the Ashtekar-Barbero components in the present paper. Note that we use the areal gauge classically, the components c and E^c is fixed at the classical level. Hence, we only need to replace Ashtekar connection component p with the corresponding holonomy. In the $\bar{\mu}$ scheme, this can be realized as $p \to \frac{1}{\delta_b} \sin(\delta_b p)$ with $\delta_b = \sqrt{\frac{\Delta}{E^c}}$ [21]. In the resulting quantum effective Hamiltonian constraints, the holonomy correction is simplified by replacing the components of Ashtekar connection p with [28]

$$p \to \frac{x}{\sqrt{\Delta}} \sin\left(\frac{\sqrt{\Delta}}{x} p\right) \tag{37}$$

after the areal gauge is imposed, where Δ is the smallest nonzero eigenvalue of the area operator [1], satisfying the equation $\Delta = 4\sqrt{3}\pi\gamma\ell_{\mathrm{Pl}}^2$, and ℓ_{Pl} represents the Planck length. The effective Hamiltonian can be constructed by replacing all the instances of p in (24) with (37) and the result is

$$\mathcal{H}_\Lambda^{(\mathrm{LQG})} = -\frac{1}{2G\gamma}\left[\frac{E^p}{\gamma x}\partial_x\left(\frac{x^3}{\Delta}\sin^2\frac{\sqrt{\Delta}p}{x} + \gamma^2 x\right) \right.$$
$$\left. -\frac{3\gamma x}{E^p} + \frac{2\gamma x^2}{(E^p)^2}\partial_x E^p - x\gamma E^p \Lambda\right]. \tag{38}$$

And we can obtain the Poisson brackets between $\mathcal{C}^{(\mathrm{LQG})}$

$$\{\mathcal{C}^{(\mathrm{LQG})}[N_1], \mathcal{C}^{(\mathrm{LQG})}[N_2]\}$$
$$= C^{(\mathrm{LQG})}\left[-\frac{x}{\gamma\sqrt{\Delta}}\sin\frac{\sqrt{\Delta}p}{x}\cos\frac{\sqrt{\Delta}p}{x}(N_1\partial_x N_2 - N_2\partial_x N_1)\right]. \tag{39}$$

Equation (22) also needs to be changed, and at the same time, in order to give desired constraint algebra (39), Eq. (22) has been modified to read as

$$N^x = -\frac{Nx}{\gamma\sqrt{\Delta}}\sin\frac{\sqrt{\Delta}p}{x}\cos\frac{\sqrt{\Delta}p}{x}. \tag{40}$$

Finally just like the classical case, once the effective Hamiltonian (38) is in hand, the modified equations of motion can be obtained

$$\dot{E}^p = -\frac{x^2}{2\gamma\sqrt{\Delta}}\partial_x\left(\frac{NE^p}{x}\right)\sin\frac{\sqrt{\Delta}p}{x}\cos\frac{\sqrt{\Delta}p}{x}, \tag{41}$$

$$\dot{p} = \frac{\gamma Nx}{2(E^p)^2}\left(1 + 2x\frac{\partial_x N}{N}\right) - \frac{\gamma N}{2x}$$
$$-\frac{N}{2\gamma\Delta x}\partial_x\left(x^3\sin^2\frac{\sqrt{\Delta}p}{x}\right) + \frac{x\gamma N\Lambda}{2}. \tag{42}$$

We now turn to solve these equations of motion in the Painlevé-Gullstrand coordinates and set $N = 1$. Taking into account the Hamiltonian constraint $\mathcal{H}_\Lambda^{(\mathrm{LQG})}$, the complete set of equations is as follows:

$$\dot{E}^p = 0, \qquad \dot{p} = 0,$$
$$N = 1, \qquad \mathcal{H}_\Lambda^{(\mathrm{LQG})} = 0. \tag{43}$$

Then by relating $\dot{E}^p = 0$ and $N = 1$, Eq. (41) implies three possibilities:

$$1, \quad \partial_x\left(\frac{E^p}{x}\right) = 0, \tag{44}$$

$$2, \quad \sin\frac{\sqrt{\Delta}p}{x} = 0, \tag{45}$$

$$3, \quad \cos\frac{\sqrt{\Delta}p}{x} = 0. \tag{46}$$

For the case 1 we assuming the term $\partial_x(\frac{E^p}{x})$ in Eq. (41) vanishes, the solutions is

$$E^p = C_3 x, \qquad (47)$$

then, by using Eq. (43), we have

$$p = \frac{x}{\sqrt{\Delta}} \arcsin\left[\left(\frac{1}{C_3^2} - 1\right)\gamma^2\Delta\frac{1}{x^2} + \frac{C_4}{x^3} + \frac{\gamma^2\Delta\Lambda}{3}\right]^{1/2}, \qquad (48)$$

where C_3 and C_4 are constants of integration. It is not hard to confirm that the solutions (47) and (48) satisfy the Hamiltonian constraint $\mathcal{H}_\Lambda^{(\mathrm{LQG})} = 0$. For cases 2 and 3, we use the same logic of [28] and, after careful calculations, it is determined that neither of them satisfies the Hamiltonian constraint. Therefore, the solution has only one form.

Next, we need to determine the values of these integration constants C_3 and C_4. Noticing Eqs. (31), (32), (47), and $N = 1$, the metric (1) can now be written in the following form

$$ds^2 = -(1 - (C_3 N^x)^2)dt^2 + 2C_3^2 N^x dx dt + C_3^2 dx^2 + x^2 d\Omega^2, \qquad (49)$$

where we should note that the LQG correction terms are present in N^x. Because we want the target metric to recover the classical case (33) when the LQG corrections are removed, it is easy to know that $C_3^2 = 1$ in this case. Substituting p (48) into N^x (40), we obtain the desired result

$$N^x = \left(\frac{x^2\Lambda}{3} + \frac{C_4}{\gamma^2\Delta x}\right)^{1/2}\left(1 - \frac{\gamma^2\Delta\Lambda}{3} - \frac{C_4}{x^3}\right)^{1/2}, \qquad (50)$$

taking into account that

$$\cos\frac{\sqrt{\Delta}p}{x} = -\sqrt{1 - \sin^2\frac{\sqrt{\Delta}p}{x}}$$

for consistency with the classical case. When $\Delta \to 0$, N^x should revert to the classical case [which can be given by using Eqs. (22) and (35)]. Hence, we can ascertain that $C_4 = 2GM\gamma^2\Delta$. Then, the resulting LQG-corrected metric with the cosmological constant reads

$$ds^2 = -F(x)dt^2 + 2N^x dx dt + dx^2 + x^2 d\Omega^2, \qquad (51)$$

with

$$F(x) = 1 - (N^x)^2, \qquad (52)$$

$$N^x = \left(\frac{x^2\Lambda}{3} + \frac{2GM}{x}\right)^{1/2}\left(1 - \frac{2GM\gamma^2\Delta}{x^3} - \frac{\gamma^2\Delta\Lambda}{3}\right)^{1/2}. \qquad (53)$$

From the above result, it can be easily verified that, as $\Delta \to 0$, the classical Schwarzschild–de Sitter(anti–de Sitter) solutions are recovered. Another point worth mentioning is that when Λ is set to zero, the metric (51) can be restored to the case without cosmological constant as that in [28], which further demonstrates the correctness of the results of the present paper. Moreover, the quantum corrected metric obtained in current paper is coincide with the metric from the quantum Oppenheimer-Snyder collapse model [42,43], which also add confidence on our model.

IV. PHYSICAL PROPERTIES OF THE EFFECTIVE METRIC

A. Geodesic and effective range

As stated in [28,43], the metric corrected by LQG is only valid for $x > x_{\min}$. This is because, in the LQC, there is an upper limit to the energy density of any matter field. Therefore, in order to generate a gravitational field with mass M, the corresponding matter field cannot be infinitely small but will have a radius corresponding to the maximum energy density. Now we will search for the lower bound $x_{\min}$.

Investigating geodesics provides a direct method for understanding the structure of spacetime, hence it is advisable to begin with them. To simplify the analysis, we will focus solely on radial geodesics that satisfy the following equation:

$$-\kappa = -F(x)\left(\frac{dt}{d\tau}\right)^2 + 2N^x\left(\frac{dx}{d\tau}\right)\left(\frac{dt}{d\tau}\right) + \left(\frac{dx}{d\tau}\right)^2, \qquad (54)$$

where τ represents the geodesic parameter. When $\kappa = 1$, it corresponds to timelike geodesics, and τ represents proper time. On the other hand, if $\kappa = 0$, it refers to null geodesics, and τ represents a chosen affine parameter. It is important to note that in this case of a stationary spherically symmetric spacetime, $T^\mu = (\partial/\partial t)^\mu$ is a Killing vector. Setting the tangent vector of the geodesic as $\xi^\mu = (\partial/\partial\tau)^\mu$, then $T^\mu\xi_\mu$ is constant along the geodesic, which we refer to as the conserved energy written as

$$E = T^\mu\xi_\mu = -F(x)\frac{dt}{d\tau} + N^x\frac{dx}{d\tau}. \qquad (55)$$

For timelike geodesics ($\kappa = 1$) and considering $E = 1$, it corresponds to a stationary particle starting its motion from infinity. The geodesic equation (54) can be further simplified as follows:

$$\frac{dx}{d\tau} = \pm\sqrt{1 - F(x)}, \qquad (56)$$

where it can be observed that $x_{\min}$ is at $dx/d\tau = 0$ and the solution is

$$x_{\min} = \left(\frac{6GM\gamma^2\Delta}{3 - \gamma^2\Delta\Lambda}\right)^{1/3}. \tag{57}$$

Compared with the Schwarzschild case [28], it is easy to see that the term involving the cosmological constant causes a slight variation on $x_{\min}$. However, when this term is neglected, we obtain exactly the same value of $x_{\min}$ as discussed in [28,44]. Moreover, since the $x_{\min}$ should be greater than zero, then the denominator of Eq. (57) implies an upper bound on the cosmological constant as $\Lambda < \frac{3}{\gamma^2\Delta}$.

Besides, for null geodesic, the situation will be much simpler. Since $\kappa = 0$, Eq. (54) can be divided by $dt/d\tau$ and written as

$$\frac{dx}{dt} = -N^x \pm 1. \tag{58}$$

A nontrivial case arises when the outgoing null rays with $dx/dt = -N^x + 1$ have zeros at $x > 0$. However, the ingoing rays with $dx/dt = -N^x - 1$ are always less than zero. One point worth mentioning here is that it is previously stated that T^a represents a Killing vector field, and its corresponding Killing horizon is given by $T^aT_a = 0$, which can be simplified as $F(x) = 0$. But in fact, since $F(x) = 0$ and $dx/dt = 0$ are equivalent to each other, the zeros of dx/dt also represent the Killing horizon.

According to [28], $M_* = 8\gamma\sqrt{\Delta}/\sqrt{27G}$ corresponding to the critical mass means that when $\Lambda = 0$ and there is only one Killing horizon. More precisely, as the mass is greater than M_*, there exist two Killing horizons, while if the mass is smaller than M_*, there are no Killing horizons. The detailed situation can be visualized in the Fig. 1.

From Fig. 2, in the case of the LQG-corrected AdS black hole, the mass exceeds M_*, resulting in the presence of both inner and outer horizons. For LQG-corrected metric, the left end point of the red curve correspond to the minimum value of x, where $dx/dt = 1$, as can be easily verified by Eqs. (52), (56), and (58). Conversely, the classical AdS black hole exhibits only one horizon, and dx/dt diverges rapidly as $x \to 0$, indicating the presence of the spacetime singularity. In the case of dS black hole, the LQG correction also results in the existence of two Killing horizons, avoiding the singularity issue. Additionally, the cosmological horizon can be observed from the curves.

B. Curvature scalars and surface gravity

Investigating the curvature of can provide us with a deeper understanding of the geometric structure of this spacetime. Furthermore, it allows for a more straightforward comparison to be made with the scenario where the cosmological constant is not present. With the corrected metric (51), various curvature scalars can be straightforwardly calculated. The results are summarized as follows:

$$R = 4\Lambda - \frac{4}{3}\gamma^2\Delta\Lambda^2 - \frac{24(GM\gamma)^2\Delta}{x^6}, \tag{59}$$
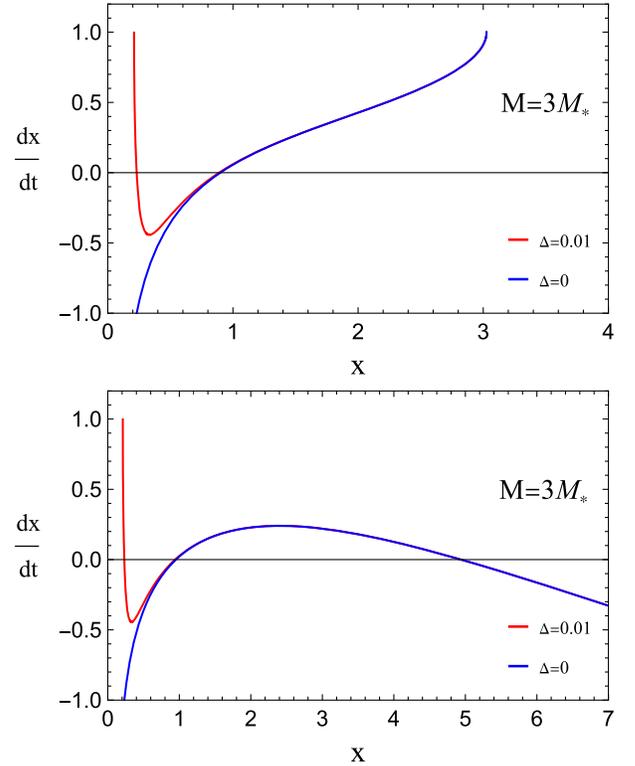
FIG. 2. For outgoing null geodesics, we have separately plotted the cases of the AdS black holes (first figure) and the dS black holes (second figure) with the mass of $3M_*$. In both figures, the red curve represents the LQG-corrected metric, while the blue curve means the classical metric. For AdS black holes, we consider $\Lambda = -0.1$, whereas for dS black holes, $\Lambda = 0.1$. All the remaining parameters are taken as $\{\gamma = 1, G = 1\}$.

FIG. 1. For outgoing null geodesics, we have plotted the case of the black hole with mass M_* and compared three different spacetimes. AdS spacetime is taken to have $\Lambda = -0.1$, while dS spacetime has $\Lambda = 0.1$. It can be observed that the three spacetimes exhibit little difference near the Killing horizon, and only significant differences arise far from the horizon. The remaining parameters are taken as $\{\gamma = 1, \Delta = 0.01, G = 1\}$.

$$R_{\mu\nu}R^{\mu\nu} = \frac{4}{9}\Lambda^2(-3+\gamma^2\Delta\Lambda)^2 + \frac{1440(GM\gamma)^4\Delta^2}{x^{12}}$$
$$+ \frac{16(GM\gamma)^2(-3+\gamma^2)\Delta\Lambda}{x^6}, \tag{60}$$

$$R_{\mu\nu\rho\sigma}R^{\mu\nu\rho\sigma} = \frac{8}{27}\Lambda^2(-3+\gamma^2\Delta\Lambda)^2$$
$$+ \frac{320(GM)^3\gamma^2(-3+2\gamma^2\Delta\Lambda)\Delta}{x^9}$$
$$+ \frac{32(GM\gamma)^2(-3+\gamma^2\Delta\Lambda)\Delta\Lambda}{x^6}$$
$$+ \frac{7488(GM\gamma)^4\Delta^2}{x^{12}}. \tag{61}$$

For physical reasons, the absolute value of curvature scalars should correspond to a maximum when x approaches $x_{\min}$ in vacuum. By substituting $x_{\min}$ into various curvature scalars, we obtain the following results

$$\lim_{x\to x_{\min}} R = -\frac{6}{\gamma^2\Delta} + 8\Lambda - 2\gamma^2\Delta\Lambda^2, \tag{62}$$

$$\lim_{x\to x_{\min}} R_{\mu\nu}R^{\mu\nu} = \frac{2(-3+\gamma^2\Delta\Lambda)^2(5-4\gamma^2\Delta\Lambda+\gamma^4\Delta^2\Lambda^2)}{\gamma^4\Delta^2}, \tag{63}$$

$$\lim_{x\to x_{\min}} R_{\mu\nu\rho\sigma}R^{\mu\nu\rho\sigma} = \frac{4(-3+\gamma^2\Delta\Lambda)^2(10-6\gamma^2\Delta\Lambda+\gamma^4\Delta^2\Lambda^2)}{\gamma^4\Delta^2}. \tag{64}$$

These are also constants independent of the black hole mass. Unsurprisingly, when the terms containing the cosmological constant are discarded, these curvature scalars align with those in [28,44].

In addition, exploring the trapped surface can further verify the results of the effective metric (51) we have obtained. Considering the null geodesic congruence, due to the spherical symmetry, on a two-dimensional sphere $\mathcal{S}$, the radial coordinate x and the time coordinate t are constant. Therefore, there are two independent null tangent vectors orthogonal to $\mathcal{S}$, referred to as outgoing null geodesics and ingoing null geodesics. These two geodesics correspond to the outgoing expansion parameter θ_+ and ingoing expansion parameter θ_-, respectively. By definition, the trapped surface corresponds to the region where both θ_+ and θ_- are negative. Here, we define the tangent vectors of the outgoing null geodesics and the ingoing null geodesics to be the same as [28], denoted by

$$l^\mu = \left(\frac{\partial}{\partial t}\right)^\mu + (1-N^x)\left(\frac{\partial}{\partial x}\right)^\mu, \tag{65}$$

and

$$k^\mu = \left(\frac{\partial}{\partial t}\right)^\mu + (-1-N^x)\left(\frac{\partial}{\partial x}\right)^\mu. \tag{66}$$

Normalize these two vector fields such that $l^\mu k_\mu = -2$ and the hypersurface metric for $\mathcal{S}$ is

$$h_{\mu\nu} = g_{\mu\nu} + \frac{1}{2}(l_\mu k_\nu + k_\mu l_\nu). \tag{67}$$

Based on the definition of the expansions θ_+ and θ_-, the simple expression can be obtained through straightforward calculations and the results are

$$\theta_+ = h^{\mu\nu}\nabla_\mu l_\nu = \frac{2}{x}(1-N^x), \tag{68}$$

$$\theta_- = h^{\mu\nu}\nabla_\mu k_\nu = -\frac{2}{x}(1+N^x). \tag{69}$$

Here, θ_- remains negative within the range of x, so considering θ_+ alone is sufficient. The main results are displayed in Figs. 3 and 4. Besides, the trapped surface tends to increase with the increase of mass. From the expression of the expansion (68) and the null geodesic (58), it can be observed that they differ only by a factor of $2/x$. Therefore, it is conceivable that the zero points of the null geodesics align with the outgoing expansion and the physical interpretation is consistent with the null geodesics.

When a black hole possesses an outer horizon, it becomes straightforward to calculate the surface gravity by employing
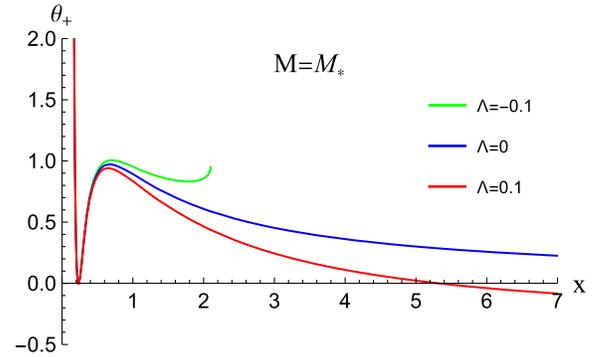
FIG. 3. The expansions of the outgoing null geodesics are compared for different cosmological constants. In this case, the mass is chosen as M_*, indicating that when $\Lambda = 0$, there is only one event horizon. More detailed calculations reveal when $\Lambda = -0.1$, there is no event horizon and the curve's end point cannot extend indefinitely but reaches a certain point. This also implies the maximum value that x can take. When $\Lambda = 0.1$, there are two close inner and outer horizons, and a cosmological horizon can be clearly observed at the end of the curve. These properties are analogous to those of the outgoing null geodesics. The remaining parameters are taken as $\{\gamma = 1, \Delta = 0.01, G = 1\}$.
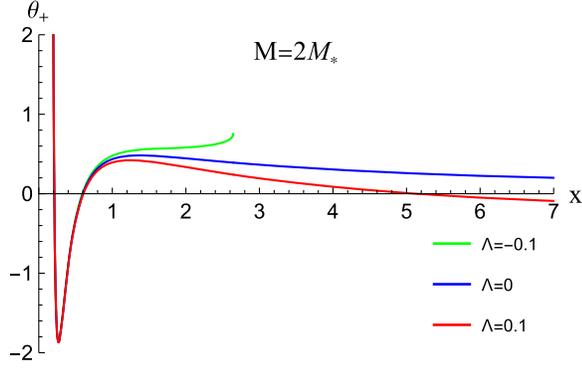
FIG. 4. Comparison of the null expansion θ_+ for the LQG-corrected metric with different values of the cosmological constant. The mass is $2M_*$, compared to the case with mass M_*, the most notable difference is that regardless of the value of the cosmological constant, the black hole exhibits both inner and outer event horizons. The influence of the cosmological constant is only evident at the end point of the curve. The remaining parameters are taken as $\{\gamma = 1, \Delta = 0.01, G = 1\}$.

$$\kappa = \frac{1}{2} \frac{\partial F(x)}{\partial x}\bigg|_{x=x_h}, \qquad (70)$$

where $x = x_h$ represents the position of the outer horizon. Due to the complexity of the expression of $F(x)$, it is not practical to calculate the analytical solution of the surface gravity directly. Moreover, if we adopt a first-order approximation for Δ, the distinctions between the three types of spacetime will not be apparent and the result of the expression will be the same. Therefore, we adopt a numerical approach to solve the problem. The detailed results are shown in Fig. 5. The green curve corresponds to the AdS black hole, and the red curve represents the dS black hole. At smaller masses, due to the LQG correction,
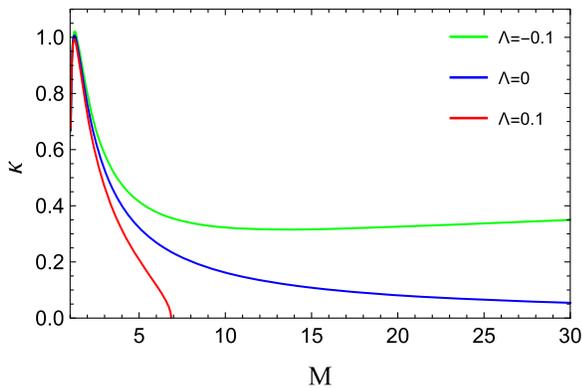
FIG. 5. By taking the mass of the black hole as the independent variable, we compared the surface gravity under different values of the cosmological constant. The mass is measured in units of M_*. The minimum value of the mass is set at M_* because when the mass is less than M_*, there is no horizon, and any discussion concerning surface gravity becomes meaningless. The remaining parameters are taken as $\{\gamma = 1, \Delta = 0.01, G = 1\}$.

they behave almost identically and both exhibit a peak. However, as the mass increases, due to the distinct characteristics of the spacetime, the surface gravity of the dS black hole rapidly tends to zero and eventually reaches an upper mass limit, whereas the surface gravity of the AdS black hole first decreases and then slowly increases.

V. THERMODYNAMICS

In LQG, the detailed study of thermodynamics is a highly active research area. Ones have successfully not only derived fundamental thermodynamic relations within the framework of effective LQC [45,46] but also obtained the Bekenstein-Hawking formula from the first principles for the Schwarzschild and other black holes [47–49]. Specifically, by applying the formalism of LQG to the statistical treatment of the microscopic degrees of freedom of black holes, an explanation for the microscopic degrees of freedom corresponding to black hole entropy has been obtained [50,51]. Unlike their approach of studying thermodynamics from the fundamental LQG formalism, we conduct a conventional analysis based on the derived effective metric.

Within this subsection, it is specified that we are adopting the natural units exclusively ($G = \hbar = c = k_B = 1$). From Eqs. (52) and (53), the mass of black holes can be expressed in terms of the outer horizon x_h,

$$M = \frac{x_h^3(3 - 2\gamma^2\Delta\Lambda) - 3x_h^2\sqrt{x_h^2 - 4\gamma^2\Delta}}{12\gamma^2\Delta}. \qquad (71)$$

The Hawking temperature of the black holes can be easily obtained by requiring the absence of conical singularity at the horizon in the Euclidean sector of the black hole solution,

$$
\begin{aligned}
T &= \frac{1}{4\pi}\frac{\partial F(x)}{\partial x}\bigg|_{x=x_h}, \\
&= \frac{-3x_h^2 + x_h\sqrt{x_h^2 - 4\gamma^2\Delta}(3 - 2\gamma^2\Delta\Lambda) + 8\gamma^2\Delta}{8\pi x_h \gamma^2 \Delta},
\end{aligned} \qquad (72)
$$

and the corresponding Fig. 6 is plotted. Interestingly, we observed that for a small black hole, the temperature of the LQG black hole decreases as the radius decreases, which is quite different with the classical scenario. However, in some modified gravity theories, the corresponding Hawking temperature also exhibits the similar behavior [52]. The heat capacity of black holes reads [53]

$$C = \left(\frac{\partial M}{\partial x_h}\right)\bigg/\left(\frac{\partial T}{\partial x_h}\right), \qquad (73)$$

and the corresponding Fig. 7 is also plotted. Figure 7 reveals that the LQG black hole exhibits an extra phase transition compared to the classical black hole.
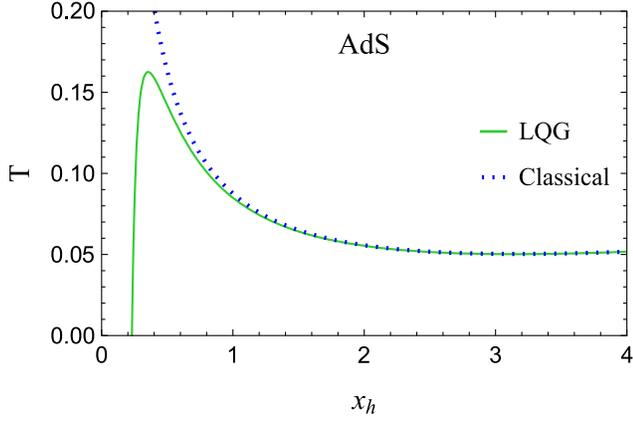
FIG. 6. $T - x_h$ diagram of two types of AdS black holes. The green solid line represents the LQG case, while the blue dashed line signifies the classical case. It indicates that when the radius is extremely small, the modification introduced by LQG does not lead to temperature divergence. The parameters are taken as $\{\gamma = 1, \Delta = 0.01, \Lambda = -0.1\}$.

Classical black holes generally satisfy the so-called area law, which states that the entropy of a black hole is equal to one-quarter of the horizon area. However, in the presence of quantum corrections, the area-entropy law no longer holds. In recent years, research within the framework of LQG has
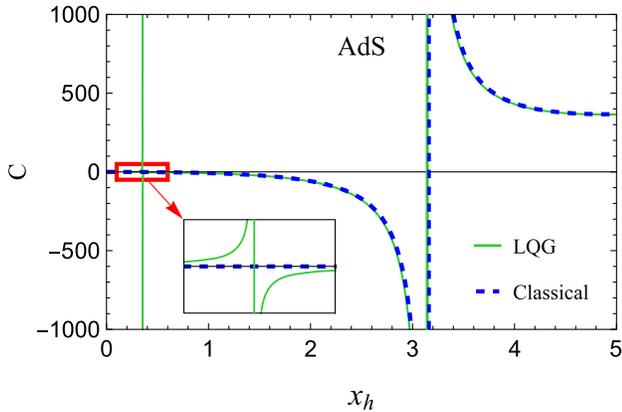
FIG. 7. $C - x_h$ diagram of two types of AdS black holes. The green vertical lines ($x \approx 0.38, x \approx 3.18$) mark the heat capacity divergence for LQG black holes, and the vertical blue dashed line ($x \approx 3.18$) does the same for classical black holes. The left green vertical line ($x \approx 0.38$), being so close to the heat capacity curve of the LQG black hole that they appear as a single vertical line. Both LQG and classical black holes exhibit a divergence in heat capacity near $x \approx 3.18$, suggesting the occurrence of a phase transition. This transition signifies a shift in thermodynamic stability from instability ($C < 0$) to stability ($C > 0$). Additionally, the magnified view in the figure reveals that the LQG black hole exhibits an extra phase transition compared to the classical black hole. At smaller horizon radius ($x < 0.38$), contrary to the classical case, the LQG black hole is stable. The parameters are taken as $\{\gamma = 1, \Delta = 0.01, \Lambda = -0.1\}$.

shown that black hole entropy, compared to the classical result, includes an additional logarithmic correction term [54,55]. We now assume that the thermodynamic first law in the extended phase space holds for our model, and thus we have [39]

$$dM = TdS + VdP. \tag{74}$$

The entropy of a black hole is

$$
\begin{aligned}
S &= \int (T^{-1}dM)_P = \int_{x_t}^{x_h} \left[T^{-1} \left(\frac{\partial M}{\partial x_h} \right) \right]_P dx_h, \\
&= \pi x_h^2 \sqrt{1 - \frac{4\gamma^2 \Delta}{x_h^2}} \\
&\quad - 2\pi\gamma^2 \Delta \ln \left(-x_h + x_h \sqrt{1 - \frac{4\gamma^2 \Delta}{x_h^2}} \right)^2 + S_0, \\
&= \frac{A}{4} + 2\pi\gamma^2 \Delta \ln \left(\frac{A}{16\pi\gamma^4 \Delta^2} \right) + S_1 + O \left[\frac{1}{x_h} \right], \tag{75}
\end{aligned}
$$

where S_0, S_1 are constants and $A = 4\pi x_h^2$. Since the entropy should approach zero as temperature nears zero, we set the lower limit of the integral to x_t, which represents the horizon radius of the black hole when the temperature vanishes. The final result employs the large black approximation such that $x_h \gg 4\gamma^2 \Delta$ holds, so the square root term can be rewritten as

$$\sqrt{1 - \frac{4\gamma^2 \Delta}{x_h^2}} = 1 - \frac{2\gamma^2 \Delta}{x_h^2} + O \left[\frac{1}{x_h} \right]^3. \tag{76}$$

Therefore, the final expression for the entropy for the large black holes can be approximately considered as being the area law plus a quantum logarithmic correction term. This is also the case for the full theories of LQG [51].

In AdS black holes, the variation of Λ can be incorporated into the first law of thermodynamics, and it is no longer treated as a constant. The pressure is understood to be a quantity related to Λ [56]:

$$P = -\frac{\Lambda}{8\pi}. \tag{77}$$

Therefore, Λ in Eq. (71) can be expressed as $-8\pi P$, and by calculating the partial derivative $\partial M / \partial P$, the thermodynamic volume of the black hole can be obtained by

$$V = \frac{4\pi x_h^3}{3}. \tag{78}$$

Utilizing Eqs. (77) and (78), the temperature (72) can be expressed in terms of variables P and V, and after rearrangement, the equation of state can be obtained by

$$P(T, V) = \frac{Q_1 + Q_2}{Q_3}, \tag{79}$$

$$Q_1 = 9\sqrt[3]{6V^2} - 16\sqrt[3]{6\pi}\gamma^2\Delta, \tag{80}$$

$$Q_2 = 3\sqrt[3]{V}(16\pi^{4/3}\gamma^2\Delta T - 3\sqrt{(6V)^{2/3} - 16\pi^{2/3}\gamma^2\Delta}), \tag{81}$$

$$Q_3 = 48\pi\gamma^2\Delta\sqrt[3]{V}\sqrt{(6V)^{2/3} - 16\pi^{2/3}\gamma^2\Delta}. \tag{82}$$

We can search for the critical point through the following conditions:

$$\left(\frac{\partial P}{\partial V}\right)_T = 0, \quad \text{and} \quad \left(\frac{\partial^2 P}{\partial V^2}\right)_T = 0. \tag{83}$$

The critical values of temperature T_c, volume V_c, and pressure P_c are given, respectively, by

$$T_c = \frac{1}{6\pi\gamma\sqrt{6\Delta}}, \tag{84}$$

$$V_c = 64\sqrt{6}\pi\gamma^3\sqrt{\Delta^3}, \tag{85}$$

$$P_c = \frac{-27 + 5\sqrt{30}}{144\pi\gamma^2\Delta}, \tag{86}$$

and we show Fig. 8 representing pressure as a function of volume. The solution has isotherms similar to the Van der Walls fluids. Having the equation of state $P(T, V)$, we can define the compressibility factor [57],

$$Z(T, V) = \frac{PV}{T}, \tag{87}$$

which indicates how much a gas deviates from ideal gases. When $Z = 1$, it implies that there is no interaction between particles. At the critical point,

$$Z_c = \frac{P_c V_c}{T_c} = 16(-27 + 5\sqrt{30})\pi\gamma^2\Delta, \tag{88}$$

which indicates that the value of Z_c is dependent on γ. Moreover, in the extended phase space, we consider that the function M play the role of enthalpy H. So, the Gibbs free energy is written as

$$G = M - TS, \tag{89}$$

and the behavior of G is shown in Fig. 9.

Critical exponents describe the behaviour of physical quantities near the critical point. It is believed that they are universal. To obtain them, we use the so-called reduced variables

$$\tilde{t} = \frac{T - T_c}{T_c}, \qquad \tilde{v} = \frac{V - V_c}{V_c}, \qquad \tilde{p} = \frac{P}{P_c}. \tag{90}$$

We define the critical exponents as α, β, λ, and χ. They are specified by the following equations,

$$C_V = T\left(\frac{\partial S}{\partial T}\right) \propto |\tilde{t}|^{-\alpha}, \tag{91}$$

$$\eta = V_1 - V_2 \propto |\tilde{t}|^{\beta}, \tag{92}$$

$$k_T = -\frac{1}{V}\frac{\partial V}{\partial P} \propto |\tilde{t}|^{-\lambda}, \tag{93}$$

$$|P - P_c| \propto |V - V_c|^{\chi}, \tag{94}$$

where C_V, η, k_T are, respectively, the heat capacity at constant volume, the difference in volume between two phases and the isothermal compressibility. Clearly, the entropy S is a function that does not explicitly depend

FIG. 8. Graphic representation of the state equation with the values $\{\gamma = 1, \Delta = 0.01, \Lambda = -0.1\}$.
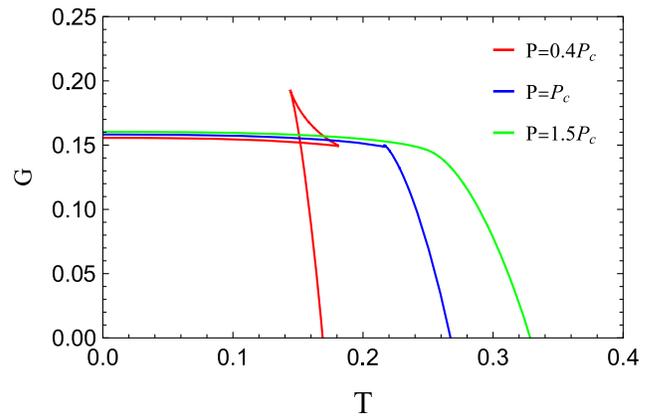
FIG. 9. This picture shows the characteristic swallowtail behavior of the Gibbs free energy as a function of temperature. It is observed that when $P < P_c$, a first-order phase transition occurs, and, at each temperature, there can be up to three values of free energy, each representing a different phase of the black hole.

on T, so it can be determined that $\alpha = 0$. If we rewrite the equation of state (79) by using Eq. (90) and expand it for small values of $\tilde{t}$ and $\tilde{v}$, we get

$$\tilde{p} = 1 + (B_1 - B_2\tilde{v})\tilde{t} - B_3\tilde{v}^3 + O(\tilde{v}^4, \tilde{t}\tilde{v}^2), \quad (95)$$

where B_1, B_2, and B_3 are positive constants. If we consider $\tilde{t}$ as constant and derive $\tilde{p}$ to $\tilde{v}$, then we obtain

$$d\tilde{p} = -(B_2\tilde{t} + 3B_3\tilde{v}^2)d\tilde{v}. \quad (96)$$

This relation is important to apply Maxwell's area law, which states [40,41]

$$\int VdP = 0. \quad (97)$$

Thus, when considering Maxwell's area law and the fact that the pressure is constant at the phase transition, we get

$$\begin{aligned}\tilde{p} &= 1 + (B_1 - B_2\tilde{v}_1)\tilde{t} - B_3\tilde{v}_1^3, \\ &= 1 + (B_1 - B_2\tilde{v}_2)\tilde{t} - B_3\tilde{v}_2^3, \quad (98)\end{aligned}$$

$$0 = \int_{\tilde{v}_1}^{\tilde{v}_2} (\tilde{v} + 1)(B_2\tilde{t} + 3B_3\tilde{v}^2)d\tilde{v}. \quad (99)$$

Solving these equations yields the nontrivial solution as follows:

$$\tilde{v}_1 = -\tilde{v}_2 = \frac{B_2}{B_3}\sqrt{-\tilde{t}} \quad \text{and thus} \quad \eta \propto \sqrt{-\tilde{t}}, \quad (100)$$

which means that one of the critical exponents is $\beta = 1/2$. We can also use Eqs. (93) and (95) to calculate the isothermal compressibility and we find that

$$k_T \propto 1/\tilde{t}, \quad (101)$$

such that $\lambda = 1$. To obtain the final critical exponents, we rewrite the condition $|P - P_c| \propto |V - V_c|^\chi$ as $|\tilde{p} - 1| \propto |\tilde{v}|^\chi$. From Eq. (95), we get

$$\tilde{p} - 1 \propto (B_1 - B_2\tilde{v})\tilde{t} - B_3\tilde{v}^3. \quad (102)$$

It is worth reminding that in the critical isotherm we have $\tilde{t} = 0$, so that,

$$\tilde{p} - 1 \propto \tilde{v}^3. \quad (103)$$

In general, the critical exponents are $\alpha = 0, \beta = 1/2$, $\lambda = 1$, and $\chi = 3$.

In general, the modifications from LQG endow vacuum spherically symmetric black holes with rich thermodynamic properties. For a small black hole, the temperature of the LQG black hole would not diverge. Moreover, the LQG corrections also introduce an extra phase transition in the black hole's heat capacity at smaller radius, suggesting that the thermodynamic properties of small black holes in LQG might be stable. The entropy of the AdS black holes in LQG shows that a logarithmic term appeared as the leading order correction to the Beikenstein-Hawking entropy. Under the premise of the first law of thermodynamics in an extended phase space (74) being valid, the $P - V$ diagram shows that AdS black holes in LQG, like Reissner-Nordström (RN)-AdS black holes [39], undergo phase transition.

VI. CONCLUSIONS AND DISCUSSIONS

The main result in this paper is obtained based on the Painlevé-Gullstrand coordinate system and utilizes the components of the Ashtekar-Barbero connection and density-triad to describe a four-dimensional spherically symmetric spacetime with a cosmological constant. We first perform calculations in the classical scenario. Starting from the gravitational action, after symmetry reduction, we consider the constrained system to consist of Hamiltonian constraint (scalar constraint) and the diffeomorphism constraint (vector constraint) due to the constrained nature of the system. By exploiting the spherical symmetry, further simplification of the constraints can be achieved. The equations of motion can then be obtained.

Then we impose a gauge fixing on the area. As a result, the number of dynamical variables is reduced from four to two, and the equations of motion are also reduced to two. By directly solving the equations, the classical Schwarzschild–de Sitter (anti–de Sitter) solutions are obtained as expected.

Next, we proceed to obtain the LQG effective dynamics for vacuum spherically symmetric spacetimes. We modified the variable p of the connection by incorporating holonomy corrections and adjusted the Hamiltonian constraint, symplectic structure, and shift vector accordingly. Similarly, by solving the modified effective equations of motion, we obtained the LQG-corrected spherically symmetric metric with a cosmological constant. In comparison with the previous treatments of LQG black hole models, our treatment leads to a significant difference. In [27], the authors investigated the quantum dynamics of the black hole interior with the cosmological constant in the unimodular gravity framework. While in our current paper, our start point is GR plus cosmological constant, we do not view the cosmological constant as a dynamical variable. As a result, analytical solutions for Schwarzschild–de Sitter (anti–de Sitter) black hole with LQG correction are obtained.

Due to the LQG correction, the variable x has a restricted range of values. For AdS and dS spacetimes, we calculated their common minimum value $x_{\min}$ using timelike geodesics. The dS spacetime exhibits the expected cosmological horizon. Compared to $\Lambda = 0$, the effect of the

cosmological constant is not only noticeable at distances far from the event horizon but also alter the geometry near the singularity. Moreover, there exist an upper bound on the cosmological constant as $\Lambda < \frac{3}{\gamma^2 \Delta}$ obtained by Eq. (57).

We also investigated the curvature scalars $R, R_{\mu\nu}R^{\mu\nu}, R_{\mu\nu\rho\sigma}R^{\mu\nu\rho\sigma}$ of the LQG-corrected metric, which are bounded at $x_{\min}$ due to quantum gravity effects and are constants that only depend on Λ and Δ. Moreover, when setting $\Lambda = 0$, all the curvature scalars can be recovered in the form presented in the article [28].

It is worth mentioning that the computation of $x_{\min}$ can also be directly obtained from $F(x)$. Since $F(x) = 1 - (N^x)^2$, it can be observed that $F(x) \leq 1$, and when $F(x) = 1$, it represents the boundary of applicability for $F(x)$. And $x_{\min}$ is one of the solutions to $F(x) = 1$.

The investigation of the thermodynamic properties of LQG black holes generally requires the premise that the first law of thermodynamics (74) holds. The quantum corrections lead to an additional logarithmic term in the entropy for large black holes, which is consistent with current results. These results are discussed within the context of a four-dimensional effective metric, but how the thermodynamic properties might change in other LQG black hole models, or whether the entropy correction also takes a logarithmic term, remains an open question worthy of further investigation.

Last but not least, for the general covariance issue, for Schwarzschild case, the quantum framework of [28] is equivalent to that in [44], and the latter is showing to be general covariance [58]. The framework of [58] can be generalized to include a cosmological constant in principle. However, since even in Schwarzschild case, the general covariance issue is still under debating [59,60], we would like to leave this topic for future study.

[1] A. Ashtekar and J. Lewandowski, Background independent quantum gravity: A status report, Classical Quantum Gravity **21**, R53 (2004).

[2] C. Rovelli, *Quantum Gravity* (Cambridge University Press, Cambridge, England, 2004).

[3] T. Thiemann, *Modern Canonical Quantum General Relativity* (Cambridge University Press, Cambridge, England, 2007).

[4] M. Han, Y. Ma, and W. Huang, Fundamental structure of loop quantum gravity, Int. J. Mod. Phys. D **16**, 1397 (2007).

[5] C. Rovelli and L. Smolin, Discreteness of area and volume in quantum gravity, Nucl. Phys. **B442**, 593 (1995).

[6] A. Ashtekar and J. Lewandowski, Quantum theory of geometry: I. Area operators, Classical Quantum Gravity **14**, A55 (1997).

[7] A. Ashtekar and J. Lewandowski, Quantum theory of geometry II: Volume operators, Adv. Theor. Math. Phys. **1**, 388 (1997).

[8] J. Yang and Y. Ma, New volume and inverse volume operators for loop quantum gravity, Phys. Rev. D **94**, 044003 (2016).

[9] T. Thiemann, A length operator for canonical quantum gravity, J. Math. Phys. (N.Y.) **39**, 3372 (1998).

[10] Y. Ma, C. Soo, and J. Yang, New length operator for loop quantum gravity, Phys. Rev. D **81**, 124026 (2010).

[11] X. Zhang and Y. Ma, Extension of loop quantum gravity to f (R) theories, Phys. Rev. Lett. **106**, 171301 (2011).

[12] N. Bodendorfer, T. Thiemann, and A. Thurn, New variables for classical and quantum gravity in all dimensions I. Hamiltonian analysis, Classical Quantum Gravity **30**, 045001 (2013).

[13] X. Zhang, J. Yang, and Y. Ma, Canonical loop quantization of the lowest-order projectable Horava gravity, Phys. Rev. D **102**, 124060 (2020).

[14] H. Tan and Y. Ma, Semiclassical states in homogeneous loop quantum cosmology, Classical Quantum Gravity **23**, 6793 (2006).

[15] M. Bojowald, Absence of a singularity in loop quantum cosmology, Phys. Rev. Lett. **86**, 5227 (2001).

[16] L. Modesto, Disappearance of the black hole singularity in loop quantum gravity, Phys. Rev. D **70**, 124009 (2004).

[17] A. Ashtekar and M. Bojowald, Quantum geometry and the Schwarzschild singularity, Classical Quantum Gravity **23**, 391 (2005).

[18] A. Ashtekar, M. Bojowald, and J. Lewandowski, Mathematical structure of loop quantum cosmology, Adv. Theor. Math. Phys. **7**, 233 (2003).

[19] M. Bojowald, Loop quantum cosmology, Living Rev. Relativity **11**, 4 (2008).

[20] A. Ashtekar and P. Singh, Loop quantum cosmology: A status report, Classical Quantum Gravity **28**, 213001 (2011).

[21] C. G. Böhmer and K. Vandersloot, Loop quantum dynamics of the Schwarzschild interior, Phys. Rev. D **76**, 104030 (2007).

[22] D.-W. Chiou, Phenomenological loop quantum geometry of the Schwarzschild black hole, Phys. Rev. D **78**, 064040 (2008).

[23] A. Ashtekar, J. Olmedo, and P. Singh, Quantum transfiguration of Kruskal black holes, Phys. Rev. Lett. **121**, 241301 (2018).

[24] C. Zhang and X. Zhang, Quantum geometry and effective dynamics of Janis-Newman-Winicour singularities, Phys. Rev. D **101**, 086002 (2020),

[25] C. Zhang, Reduced phase space quantization of black holes: Path integrals and effective dynamics, Phys. Rev. D **104,** 126003 (2021).

[26] X. Zhang, Loop quantum black hole, Universe **9,** 313 (2023).

[27] F. Sartini and M. Geiller, Quantum dynamics of the black hole interior in LQC, Phys. Rev. D **103,** 066014 (2021).

[28] J. G. Kelly, R. Santacruz, and E. Wilson-Ewing, Effective loop quantum gravity framework for vacuum spherically symmetric spacetimes, Phys. Rev. D **102,** 106024 (2020).

[29] J. Friemann, M. Turner, and D. Huterer, Dark energy and the accelerating Universe, Annu. Rev. Astron. Astrophys. **46,** 385 (2008).

[30] N. Benerjee and D. Pavon, Cosmic acceleration without quintessence, Phys. Rev. D **63,** 043504 (2001).

[31] S. Sen and A. A. Sen, Late time acceleration in Brans-Dicke cosmology, Phys. Rev. D **63,** 124006 (2001).

[32] L. Qiang, Y. Ma, M. Han, and D. Yu, 5-dimensional Brans-Dicke theory and cosmic acceleration, Phys. Rev. D **71,** 061501(R) (2005).

[33] P. J. E. Peebles and Bharat Ratra, The cosmological constant and dark energy, Rev. Mod. Phys. **75,** 559 (2003).

[34] S.-H. Henry Tye and Ira Wasserman, Brane world solution to the cosmological constant problem, Phys. Rev. Lett. **86,** 1682 (2001).

[35] S. Weinberg, The cosmological constant problem, Rev. Mod. Phys. **61,** 1 (1989).

[36] A. Ashtekar, B. Bonga, and A. Kesavan, Gravitational waves from isolated systems surprising consequences of a positive cosmological constant, Phys. Rev. Lett. **116,** 051101 (2016).

[37] J. M. Bardeen, B. Carter, and S. W. Hawking, The four laws of black hole mechanics, Commun. Math. Phys. **31,** 161 (1973).

[38] R. M. Wald, The thermodynamics of black holes, Living Rev. Relativity **4,** 6 (2001).

[39] D. Kubiznak and R. B. Mann, P-V criticality of charged AdS black holes, J. High Energy Phys. 07 (2012) 033.

[40] Z. Dayyani, A. Sheykhi, M. H. Dehghani, and S. Hajkhalili, Critical behavior and phase transition of dilaton black holes with nonlinear electrodynamics, Eur. Phys. J. C **78,** 1 (2018).

[41] S.-W. Wei and Y.-X. Liu, Extended thermodynamics and microstructures of four-dimensional charged Gauss-Bonnet black hole in AdS space, Phys. Rev. D **101,** 104018 (2020).

[42] C.-Y. Shao, C. Zhang, W. Zhang, and C.-G. Shao, Scalar fields around a loop quantum gravity black hole in de Sitter spacetime: Quasinormal modes, late-time tails and strong cosmic censorship, Phys. Rev. D **109,** 064012 (2024).

[43] J. Lewandowski, Y. Ma, J. Yang, and C. Zhang, Quantum Oppenheimer-Snyder and Swiss Cheese models, Phys. Rev. Lett. **130,** 101501 (2023).

[44] R. Gambini, J. Olmedo, and J. Pullin, Spherically symmetric loop quantum gravity: Analysis of improved dynamics, Classical Quantum Gravity **37,** 205012 (2020).

[45] L.-F. Li and J.-Y. Zhu, Thermodynamics in loop quantum cosmology, arXiv:0812.3544.

[46] X. Zhang, Thermodynamics in new model of loop quantum cosmology, Eur. Phys. J. C **81,** 117 (2021).

[47] M. Domagala and J. Lewandowski, Black-hole entropy from quantum geometry, Classical Quantum Gravity **21,** 5233 (2004).

[48] A. Ashtekar, J. Engle, and C. V. D. Broeck, Quantum horizons and black-hole entropy: Inclusion of distortion and rotation, Classical Quantum Gravity **22,** L27 (2005).

[49] S. Song, G. Long, C. Zhang, and X. Zhang, Thermodynamics of isolated horizons in loop quantum gravity, Phys. Rev. D **106,** 126007 (2022).

[50] A. Ghosh and A. Perez, Black hole entropy and isolated horizons thermodynamics, Phys. Rev. Lett. **107,** 241301 (2011).

[51] J. F. Barbero G. and D. Pranzetti, Black hole entropy in loop quantum gravity, in *Handbook of Quantum Gravity*, edited by C. Bambi, L. Modesto, and I. Shapiro (Springer Nature, Singapore, 2023), pp. 1–28.

[52] Y. Huang, D. Liu, and H. Zhang, Novel black holes in higher derivative gravity, J. High Energy Phys. 02 (2023) 057.

[53] R.-G. Cai, Gauss-Bonnet black holes in AdS spaces, Phys. Rev. D **65,** 084014 (2002).

[54] E. Frodden, A. Ghosh, and A. Perez, Black hole entropy in LQG: Recent developments, AIP Conf. Proc. **1458,** 100 (2012).

[55] J. Diaz-Polo, Isolated horizons and black hole entropy in loop quantum gravity, SIGMA **8,** 048 (2012).

[56] D. Kastor, S. Ray, and J. Traschen, Enthalpy and the mechanics of AdS black holes, Classical Quantum Gravity **26,** 195011 (2009).

[57] M. E. Rodrigues and H. A. Vieira, Bardeen solution with a cloud of strings, Phys. Rev. D **106,** 084015 (2022).

[58] R. Gambini, J. Olmedo, and J. Pullin, Towards a quantum notion of covariance in spherically symmetric loop quantum gravity, Phys. Rev. D **105,** 026017 (2022).

[59] M. Bojowald, Comment on "Towards a quantum notion of covariance in spherically symmetric loop quantum gravity," Phys. Rev. D **105,** 108901 (2022).

[60] R. Gambini, J. Olmedo, and J. Pullin, Reply to "Comment on 'Towards a quantum notion of covariance in spherically symmetric loop quantum gravity'", Phys. Rev. D **105,** 108902 (2022).